Telescope simulator for the Nexus wavefront control testbed

Andrew E. Lowman[a], Fang Shi[a], David C. Redding[a], Scott A. Basinger[a],
Charles W. Bowers[b], Pamela S. Davila[b]

[a]Jet Propulsion Laboratory (JPL), California Institute of Technology, Pasadena, CA 91109
[b]NASA Goddard Space Flight Center (GSFC), Greenbelt, MD 20771

ABSTRACT

A telescope simulator was built as part of the Nexus wavefront control testbed, an NGST technology experiment at NASA's Goddard Space Flight Center. This testbed was designed to demonstrate complete control of a segmented telescope, from initial capture of light, through coarse alignment and phasing, to fine phasing and wavefront control. The existing telescope simulator allows testing of the fine phasing and wavefront control steps. A small deformable mirror in the simulator allows generation of an unobscured aberrated wavefront, for use in exploring the range of measurement and correction using the testbed's image-based wavefront sensor and larger deformable mirror. An alternate path under development for the simulator will create a segmented wavefront using three spherical mirrors; three-degree-of-freedom mounts under each mirror enable alignment and phasing experiments that will cover most of the operation sequence. Details of the hardware design and performance will be presented.

Keywords: NGST, space optics, active optics, wavefront sensing, deformable mirror, segmented aperture

1. INTRODUCTION

The "yardstick" design for the Next Generation Space Telescope (NGST) utilizes the science camera to provide all the information needed by alignment and control operations.[1,2] The Developmental Comparative Active Telescope Testbed (DCATT) was initiated at Goddard Space Flight Center (GSFC) to demonstrate the feasibility of controlling a segmented telescope using only focal plane-based measurements rather than separate wavefront sensors or metrology beams.[3-6] DCATT was recently refocused to support the Nexus space telescope project.[7] One key element of the testbed is a telescope simulator.

The DCATT telescope simulator was originally envisioned as a means of conducting experiments on a contiguous wavefront before the segmented telescope was integrated. The simulator would also provide a variable aberration generator for testing the system deformable mirror (DM) and a measured piston source for calibrating and testing the dispersed fringe sensor (DFS) in the back end of the system.[8] All of these functions have been successfully implemented. Recent work has focused on enabling phasing experiments on a segmented wavefront. Details of the telescope simulator design and performance will be presented.

2. BACKGROUND – YARDSTICK AND DCATT

The NGST "Yardstick" is a point design developed by a NASA team led by GSFC.[1] Its purpose is to help in evaluating feasibility and expected performance for NGST, identify technology development requirements, and to prepare the project for the procurement of the NGST system. The Yardstick consists of a three-mirror telescope, with an 8-meter primary mirror (PM) containing nine segments, one center segment and eight petals in a "flower" configuration. The tertiary mirror relays the exit pupil of the telescope to a deformable mirror, which corrects any residual PM figure error and aberration remaining after the segments and secondary mirror (SM) have been aligned. Images from the near infrared camera are used to calculate all control signals sent to the telescope and deformable mirror actuators; a dedicated wavefront sensor was deemed unnecessary and too expensive for the cost constrained environment of NGST.

Extensive modeling of the Yardstick has included development of a complete operation sequence for the deployment and alignment of the telescope. All measurements will use a bright unresolved star selected by the star tracker. After initial deployment of the segments, it is likely that no light from the star will fall on the science camera; effectively, the wavefront error may be on the order of millimeters. Each segment is scanned in an increasing conical pattern until light from that segment falls on the focal plane. Each spot, which may be badly defocused and aberrated, is moved to a predetermined location. At this point, the wavefront error can be on the order of 100's of ~~microns~~. Each segment is individually focused using an encircled energy metric. The wavefront error will then be on the order of 10's of microns, limited by the diffraction limited depth of focus of the individual segments.

Two complementary techniques, dispersed fringe sensing and white light interferometry, are used for coarse phasing. One segment, for example the center segment, is chosen as a reference. The spot from another segment is overlaid onto the reference spot, and a dispersed fringe sensor (DFS) is inserted into the beam. The DFS is a prism or grism that simply disperses the light from the segments. A bright spot appears at those points where the optical path difference (OPD) between the segments is an integral number of wavelengths; a dark spot appears where the OPD is a half-integral number of wavelengths. The result is a fringe pattern whose period is inversely proportional to the piston between the segments.[8] The segment under evaluation is pistoned to remove this difference. All segments may be phased pairwise with the reference, or overlapped sequentially. The DFS takes the wavefront error from 10's of microns to less than 1 micron. White light interferometry, also referred to as image sharpening, is simply an analysis of the image formed by overlapping segments. Each segment is sequentially scanned in piston with respect to the reference while observing the peak signal and then moved to the location of the peak. This method reduces the wavefront error to the order of 100 nanometers. In the event that a DFS is not used, either by choice or a failure in its mechanism, white light interferometry may be used for the entire coarse phasing operation. However, the dynamic range of this approach is much smaller than that of the DFS, so the segments would have to be blindly scanned in piston until a useful signal is acquired.

The residual wavefront error after coarse phasing is measured and removed using a fine phasing and wavefront control step. Focus-diverse phase retrieval is the baseline wavefront sensing technique.[2] A focus mechanism or weak lens in a filter wheel is used to generate defocus, and four or more images are recorded at different defocus positions. An iterative Fourier transform algorithm is combined with a model of the system to process the data. The resulting wavefront measurement is used to compute a correction signal using an optimal control law, which is then applied to both the PM segment actuators and the DM actuators to correct the wavefront. A final phase retrieval measurement will confirm the correction.

To demonstrate this operation sequence and the use of phase retrieval in a wavefront sensor, the DCATT testbed was undertaken. DCATT was to demonstrate alignment and control of a segmented telescope using only image-based measurements and to investigate the issues and limitations of such an approach. The bulk of the testbed was constructed at GSFC and became operational in 1999. All functions are remotely commanded over the Internet, currently by machines at GSFC and JPL. A layout of DCATT is shown in Figure 1. A source module provides point source illumination for the system. Inside the source are a laser and white light (Xenon) lamp. Neutral density filters and a rotating polarizer allow control of the laser beam power, while neutral density and spectral filters allow control of the white light beam power and wavelength. Light from the pinhole is reflected off a beamsplitter on its way to a telescope or telescope simulator and transmitted on its return trip toward a set of relay optics, referred to as the aft optics.

The aft optics consist of a pair of off-axis paraboloids (OAP's), fold mirrors, a deformable mirror (DM), and wavefront sensor components. The incoming beam is collimated by the first OAP, which also images the exit pupil of the telescope/simulator onto the Xinetics 349-actuator DM, referred to as the system DM. Another OAP focuses the beam onto a scientific grade CCD mounted on a motorized translation stage. The DFS is mounted on another motorized stage. A lens in a filter wheel is used to image the pupil onto the CCD, providing a measurement of the pupil illumination profile for incorporation into the phase retrieval algorithm. Such a measurement is important for use with a laboratory source, since diffraction from the source pinhole will generate a beam that may be far from uniform.

DCATT was to include a meter-class segmented telescope, but slow progress in polishing the aluminum PM and extensive problems with the actuators led to significant schedule delays. A decision was made to halt work on the telescope and refocus the testbed toward the success of Nexus. The original DCATT telescope simulator module already provided a basis for experiments with the testbed, while a pending upgrade to the simulator will allow a faster path to investigating many of the phasing operations that were envisioned for the telescope.

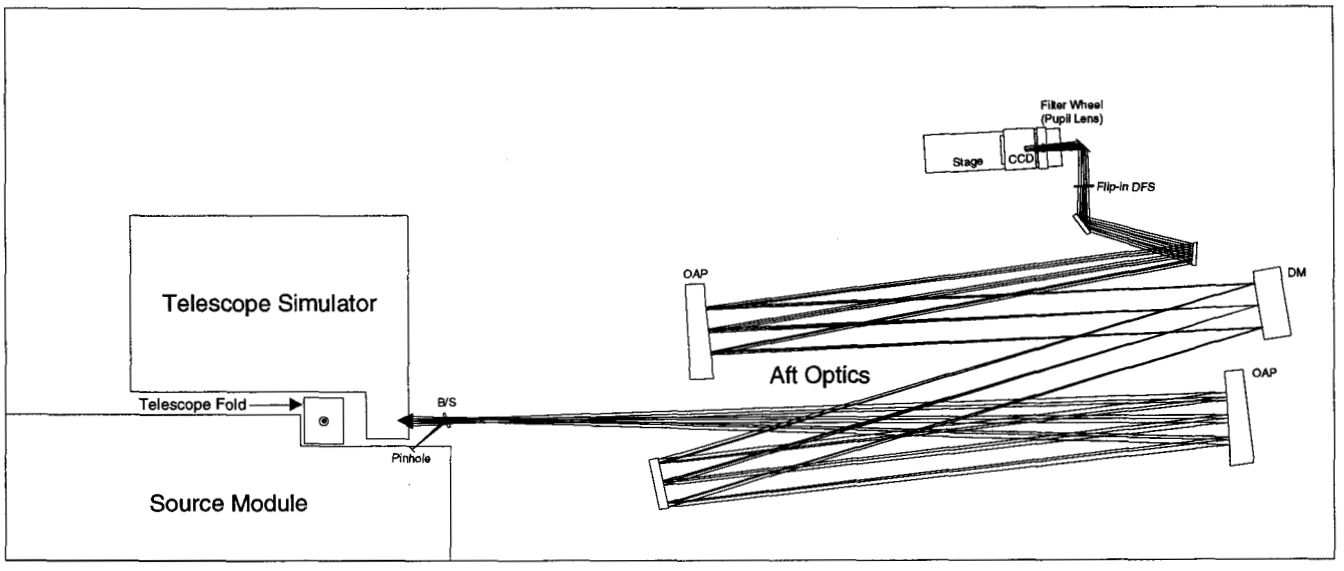

Figure 1. DCATT testbed.

3. TELESCOPE SIMULATOR DESIGN

The purpose of the DCATT telescope simulator was to provide a test path for use before the telescope was integrated, as well as a means of generating a wavefront with a variable level of aberration. A layout is shown in Figure 2. A motorized flip-in mirror bypasses the telescope path and directs the beam into the simulator. An OAP collimates the beam and sends it through a fold to a small deformable mirror. The beam is normal to the DM and autoreflects onto itself. A motorized filter wheel between the fold and DM is used to insert phase plates, windows with a step function etched onto them. Another mirror on a motorized mount allows the DM to be bypassed, if desired.

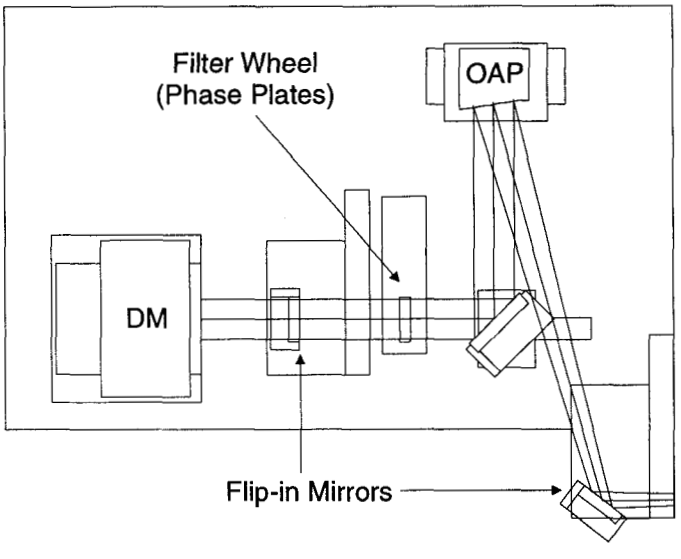

Figure 2. Layout of the current telescope simulator.

A small DM is used to generate aberrations as well as enabling some wavefront control experiments. This elements is an Itek 97 actuator DM originally built for a Department of Defense experiment in the late 1980's. The actuator spacing is 7mm. Custom electronics were built at JPL for a different experiment and provide a maximum stroke of 2.6μm. The beam diameter on the DM is 46mm. Only 32 actuators fall within the clear aperture, while 52 have an influence on the wavefront. The actuator-to-actuator spacing has been limited to 1μm difference in software to avoid overstressing the thin mirror. A further limit is placed by one bad actuator, just outside the clear aperture, which is frozen at its zero voltage position. Coupled with the number of actuators across the beam, these limits restrict the DM to generating low-order aberrations with a couple microns of wavefront error. The surface figure of the DM is 0.23λ PV and 0.033λ rms over the used clear aperture when no voltage is applied to the actuators.

The phase plates provide a known amount of piston for calibration and testing of the DFS. These plates were made by Rochester Photonics. These 2" diameter fused silica substrates contain steps fabricated by masking one half and etching the other half. Four phase plates are in the filter wheel, providing step sizes of 0.5, 2.5, 5.0, and 10.0μm.

Excluding the DM, the only powered optic in the simulator is a Zerodur OAP, manufactured by Lambda Ten (now part of McPherson). The 30" focal length was chosen to use as much of the simulator DM as possible while sticking to commonly stocked values to minimize lead time. The surface figure error was measured to be 0.012λ rms over the used clear aperture. The OAP-to-DM separation was set so that the simulator DM is imaged onto the system DM in the aft optics. The flip-in and fold mirrors are stock Zerodur mirrors with λ/20 PV surface figure.

4. TELESCOPE SIMULATOR PERFORMANCE

The final simulator wavefront error was nearly diffraction limited in double pass. The expected double pass wavefront from the simulator, calculated by taking a root-sum-square (RSS) combination of the measured figure errors of the flat mirrors, OAP, and simulator DM, was 0.086λ rms. The simulator was aligned to the DCATT aft optics by adjusting its OAP and measuring the wavefront with a Zygo GPI interferometer. The final measurement yielded a double pass value of 0.088λ rms. Considering that the aft optics alone gave a double pass interferometric measurement of 0.080λ rms, it is clear that the alignment process has partially compensated for astigmatism on the mirror surfaces with astigmatism from the alignment of the simulator OAP. A slightly lower wavefront error may have been obtained if not for the effect of jitter on the interferometer.

Influence functions were measured for the simulator DM to enable wavefront flattening, as well as to provide a more accurate means of generating aberrations. Measurements were done for each actuator by poking the actuator, measuring the wavefront using the DCATT wavefront sensor and phase retrieval, and subtracting the nominal wavefront measured by the same technique. The influence functions were then utilized to flatten the wavefront using the simulator DM. This was done initially before the larger system DM was integrated. A phase retrieval measurement of the system in this state with the simulator DM floating at its nominal level is shown in Figure 3A. The wavefront error is 0.081λ rms. The wavefront flattened using the simulator DM is shown in Figure 3B and has a wavefront error of 0.028λ rms.

The simulator has been successfully used to generate an aberrated wavefront and to generate fringes with the DFS. Figure 4 shows a wavefront containing several waves of astigmatism. Figure 5 shows an image using the DFS with the 10μm-step phase plate. These fringes agree well with modeling results.[8] This image has been processed to remove the signal variation as a function of wavelength, which is significant when using a Xenon lamp.

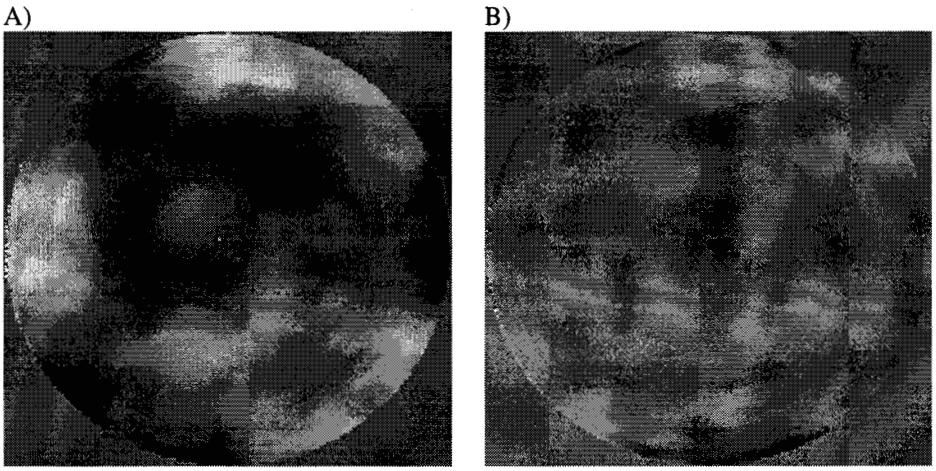

Figure 3. Wavefront with A) simulator DM floating (0.081λ rms), and B) simulator DM flattened (0.028λ rms)

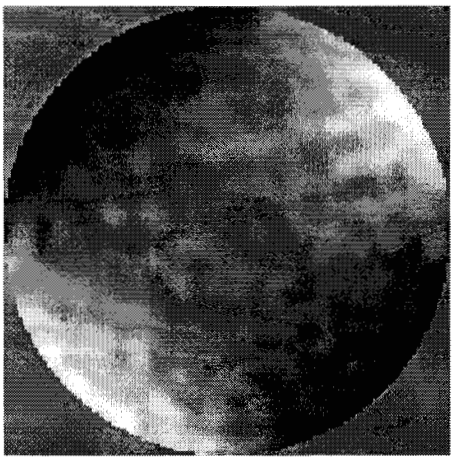

Figure 4. Wavefront showing 1λ PV astigmatism on simulator DM.

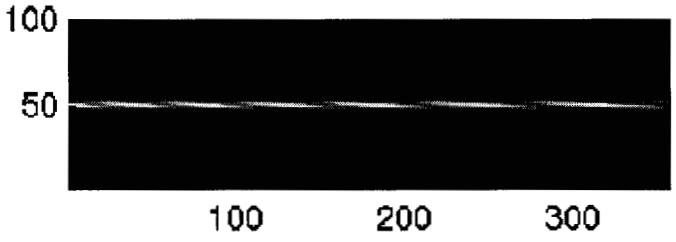

Figure 5. Dispersed fringe sensor image with 10μm phase plate.

5. TELESCOPE SIMULATOR UPGRADE

Modifications in work will allow phasing experiments using the telescope simulator. The focus of this effort has been to rapidly implement the changes by using off-the-shelf parts as much as possible and fitting them into the existing telescope simulator module. As of March 2000 the parts are in the process of integration and experiments will commence shortly. Extensive modeling has already been performed on the subsystem in preparation of first light.[9]

The new layout for the simulator is shown in Figure 6. The normal-incidence DM bypass mirror has been replaced by a tilted flip-in mirror to send the beam along a different path, through other folds and a second OAP. This OAP focuses the beam to the center of curvature of a cluster of three spherical segments. The flip-in-to-OAP separation is set to place the segmented optics at a surface conjugate to the simulator DM, so that they too will be imaged onto the system DM. As before, all of the optics have $\lambda/20$ PV surface figure, with the exception of the spheres, which had catalog specs of $\lambda/10$ PV and were measured at $\lambda/15$ PV.

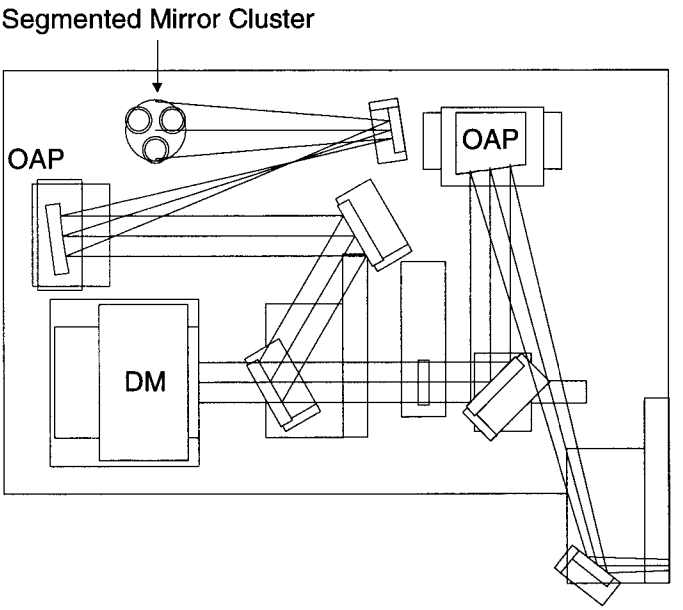

Figure 6. Layout of the upgraded telescope simulator.

The heart of the simulator upgrade is a cluster of segmented optics. A solid model is shown in Figure 7. Three spherical mirrors are held in cells sitting atop pairs of stacked actuator platforms. The top platform uses three PZT's to provide ±6μm of fine control, while the bottom platform uses three New Focus picomotors to give ±1.5mm of coarse control. Most of the parts are made of invar.

The PZT platforms are closed-loop devices from Physik Instrumente. The platforms contain PZT's and strain gauges which coupled with dedicated electronics provide automatic correction for any changes as a result of temperature drifts or hysteresis. The catalog closed-loop resolution is stated as 0.2nm, though changes in the strain gauge readings of ±1-2nm have been observed. Heating a platform resulted in a noticeable change in voltage, but a constant position was maintained. The PZT electronics have a dynamic mode that takes as input a table of numbers for each actuator, enabling dynamic behavior. This mode will be used to introduce jitter to the segments, both line of sight jitter by coupling the position changes and differential jitter to give segment-to-segment changes. The throw of the PZT's is 12μm. This allows fine tilt control over a range of only ±109 pixels on the CCD, insufficient to get the light off the focal plane. The no-light situation can be simulated by reading only a small window of pixels on the CCD, such as 32X32, but the range of the PZT's would still be much too small to defocus the segments.

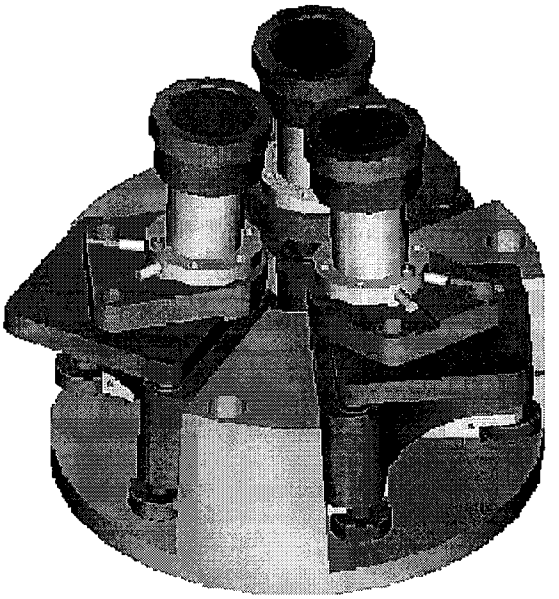

Figure 7. AutoCAD model of the segmented optics cluster.

The New Focus picomotor mounts provide coarse control that enables the segments to be defocused. While the contiguous beam is f/5.8 at the spheres, each individual segment is f/19.2. For the nominal operating wavelength of 632.8nm, this gives a diffraction limited depth of focus of ±467μm, much larger than the throw of the PZT's. The picomotors provide up to 12mm of motion, though the range has been restricted to ±1.5mm for this application. Picomotors are compact devices that use a PZT to drive a screw by leveraging the difference between dynamic and static friction. Their pulse size was measured to be nominally 17nm, though this varied by 15-20% at different actuator positions and between actuators. The pulse size will also change as a function of load, temperature, and probably time. This behavior will have to be factored into the control, unless a compact measurement device such as a fiber optic position sensor is used. Other types of motorized stages are more predictable and repeatable, but take up much more space than was available. The coarse stages also provide sufficient tilt to get light completely off the focal plane.

Thermal behavior of the segments is a critical concern, especially material expansion due to small segment-to-segment temperature changes. To mitigate these effects, all custom parts in the segmented optics cluster are made of invar. Expansion of the stainless steel housing for the PZT's will be compensated for by closed-loop control of the PZT's. Expansion of the aluminum New Focus mount has been factored into the simulator error budget. 0.1K was assumed as a reasonable segment-to-segment difference based on short-term behavior measured with the DCATT actuators. Concerns about heating from the picomotors led to thermal characterization of one set of New Focus actuators. Driving one actuator for one minute, which will take the actuator from the center to edge of its dynamic range (or vice versa), raised the temperature 0.1K before stabilizing after 15 minutes. Driving three actuators for one minute raised the temperature 0.3K before stabilizing, again after 15 minutes. During the test the mounts were supported by a thin piece of aluminum, so thermal conductance off the mounts was poor. The assembled cluster will have significantly better conductance, so thermal behavior should be much improved. Since the picomotors will only run before coarse phasing, and the coarse phasing operations will take longer than the 15 minutes required for the temperature to stabilize, the heat from the picomotors should have little effect on the critical fine phasing operation.

Initially the spherical mirrors will have nearly identical curvatures, but the cluster was designed to easily allow these to be replaced with different mirrors. The mirrors have a nominal radius of curvature of 400mm, chosen based on an available OAP focal length and the need to image the segmented optics onto the system DM. Seven off-the-shelf fused silica spheres were purchased from CVI with the hope that at least three of them would come from the same polishing run and have nearly identical curvatures. Measurements showed that five spheres had one curvature while the other two had a different one, to within the ±38μm accuracy of the photogrammetric technique used. The cells for the mirrors were designed to be easily

switched, so that eventually the effect of radius of curvature mismatch can be explored by inserting spheres with slightly different curvatures. The standard variation in CVI's catalog values for this particular curvature is ±0.1%, insufficient to have a noticeable effect, so a custom polishing run will be needed with additional polishing time given to some parts to significantly change their curvatures.

The segmented optics upgrade to the simulator will provide the functionality needed to explore many of the yardstick NGST alignment and control steps. These include initial capture, starting with no light on the focal plane; segment focus, starting with each segment out of focus; dispersed fringe sensing to phase the segments; white light interferometry to improve phasing of the segments; fine phasing via wavefront measurement using phase retrieval; and wavefront control using the segmented mirror and DM actuators. The improved simulator will not provide exploration of SM alignment; six degrees of freedom on the segments; field dependence; or figure control on segments, other than radius of curvature mismatch. Further enhancements to the Nexus wavefront control testbed may enable some of these issues to be explored.

6. CONCLUSION

A telescope simulator was constructed for the DCATT/Nexus testbed. A small deformable mirror allows generation of a contiguous aberrated wavefront with several microns of wavefront error, and phase plates provide a calibrated amount of piston for use with the dispersed fringe sensor. The hardware has performed well, and resulting images were presented. An upgrade effort will add three spherical segments, each mounted on three-axis PZT and picomotor platforms. The improved simulator will allow capture, alignment, and phasing experiments, in addition to fine phasing and wavefront control, and will help validate the NGST yardstick operation sequence.

7. ACKNOWLEDGMENTS

The authors wish to thank Randy Hein and Bob Debusk for support in mechanical design, fabrication, and assembly at JPL; John Hagopian, Todd Norton, and Peter Petrone for help in integrating the telescope simulator into the testbed at GSFC; and Jennifer Deering and Ladd Wheeler for assistance in control software development.

Research described in this publication was carried out at the Jet Propulsion Laboratory, California Institute of Technology, under contract with the National Aeronautics and Space Administration.

7. REFERENCES

1. D. C. Redding, S. A. Basinger, A. E. Lowman, A. Kissil, P. Y. Bely, R. Burg, R. G. Lyon, G. E. Mosier, M. Femiano, M. E. Wilson, R. G. Schunk, L. Craig, D. N. Jacobson, J. Rakoczy, J. B. Hadaway, "Wavefront sensing and control for a Next Generation Space Telescope" Proc. Soc. Photo-Opt. Instrum. Eng. **3356**, 758-772 (1998).
2. D. C. Redding, S. A. Basinger, A. E. Lowman, F. Shi, P. Y. Bely, R. Burg, C. W. Bowers, L. Burns, P. S. Davila, M. W. Fitzmaurice, G. E. Mosier, B. D. Perkins, "Wavefront control for a segmented deployable space telescope" Proc. Soc. Photo-Opt. Instrum. Eng. **4013** (2000).
3. D. R. Coulter, "Technology development for the Next Generation Space Telescope: an overview," Proc. Soc. Photo-Opt. Instrum. Eng. **3356**, 106-113 (1998).
4. C. M. LeBoeuf, P. S. Davila, D. C. Redding, A. Morell, A. E. Lowman, M. E. Wilson, E. W. Young, L. K. Pacini, D. R. Coulter, "Developmental Cryogenic Active Telescope Testbed: a wavefront sensing and control testbed for the Next Generation Space Telescope," Proc. Soc. Photo-Opt. Instrum. Eng. **3356**, 1168-1178 (1998).
5. P. S. Davila, A. E. Lowman, M. E. Wilson, R. A. Boucarut, C. M. LeBoeuf, D. C. Redding, E. W. Young, "Optical design of the Developmental Cryogenic Active Telescope Testbed," Proc. Soc. Photo-Opt. Instrum. Eng. **3356**, 141-152 (1998).
6. E. W. Young, M. E. Wilson, P. S. Davila, W. L. Eichhorn, C. M. LeBoeuf, D. C. Redding, A. E. Lowman, "Performance analysis of the Developmental Cryogenic Active Telescope Testbed," Proc. Soc. Photo-Opt. Instrum. Eng. **3356**, 161-175 (1998).

7. R. Burg, J, Burt, H. Bremmer, J. Lawrence, A. E. Lowman, C. M. Perrygo, K. Parrish, D. C. Redding, A. Morell, J. G. Hagopian, C. M. LeBoeuf, P. K. Shu, R. Doxsey, R. W. Mollerick, "Nexus flight experiment concept," Proc. Soc. Photo-Opt. Instrum. Eng. **4013** (2000).
8. F. Shi, D. C. Redding, S. A. Basinger, A. E. Lowman, C. W. Bowers, P. S. Davila, M. E. Wilson, T. Norton, P. Petrone, "DCATT Dispersed Fringe Sensor: modeling and experimenting with the transmissive phase plates," Proc. Soc. Photo-Opt. Instrum. Eng. **4013** (2000).
9. S. A. Basinger, D. C. Redding, A. E. Lowman, L. Burns, D. Cohen, K. Y. Liu, "Performance of wavefront sensing and control algorithms on a segmented telescope testbed," Proc. Soc. Photo-Opt. Instrum. Eng. **4013** (2000).